The effect of well coupling on effective masses in the InGaAsN material system

2007 J. Phys.: Condens. Matter 19 276202

(http://iopscience.iop.org/0953-8984/19/27/276202)

IOP PUBLISHING JOURNAL OF PHYSICS: CONDENSED MATTER

J. Phys.: Condens. Matter **19** (2007) 276202 (8pp) doi:10.1088/0953-8984/19/27/276202

The effect of well coupling on effective masses in the InGaAsN material system

M S Wartak and P Weetman

Department of Physics and Computer Science, Wilfrid Laurier University, Waterloo, ON, N2L 3C5, Canada

Received 23 May 2007
Published 20 June 2007
Online at stacks.iop.org/JPhysCM/19/276202

Abstract

The effect of well coupling on effective masses for InGaAsN based heterostructures is numerically analysed. The analysis is based on the 10×10 Luttinger–Kohn Hamiltonian which couples valence, conduction and nitrogen bands. Our results show that by adjusting the nitrogen composition and/or the barrier width, effective masses can be effectively modified.

1. Introduction

InGaAsN based structures have been studied extensively in recent years as a candidate for quantum well (QW) based semiconductor lasers emitting light at a wavelength of 1.3 μm [1]. Recently there have been several theoretical analyses published [2–4] on the material gain, differential gain and linewidth enhancement factor for GaInNAs/GaAs single quantum wells based on the free-carrier theory. In our previous work we explored the effect of nitrogen composition on peak differential gain and transparency concentration. The linewidth enhancement factor was found to have similar values than those of the conventional material InGaAsP/InP, which is encouraging for the use of InGaAsN as the active material in a high speed emitter.

It is known that coupling between quantum wells significantly affects the operation of multiple quantum well (MQW) devices. Theoretical analysis of coupling effects on such properties as optical gain, differential gain and electric field induced refractive index have been performed for GaAs/AlGaAs based devices [5–8]. It was shown that well coupling substantially shifts the spectral gain peak and band mixing reduces the gain peak. Differential gain for narrow quantum wells is enhanced for barriers within the range of 20–50 Å, depending on carrier concentration.

Another key property is the effective masses of carriers close to band-edges. Theoretical studies of the electron masses in $In_xGa_{1-x}As_{1-y}N_y$/GaAs single quantum wells using the 10×10 Hamiltonian have been reported and compared with experimentally determined effective masses [9]. Numerical analysis of the effective masses of holes in InGaAsN single quantum well structures with self-consistent effects were reported recently by us [3]. Related

theoretical and experimental studies of $GaAs_{1-y}N_y$/GaAs quantum well systems have also been performed [10, 11].

In the present paper we report on first findings of the effective masses of carriers of two coupled wells fabricated from InGaAsN. We follow the procedures described in recent papers [3, 9] and perform numerical simulations for a range of separation barrier widths and nitrogen compositions. In section 2 we describe our theory and in section 3 we present our results.

2. Theory

2.1. Band structure

To calculate the electron and hole band structures of the quantum well, we use a plane-wave expansion method which assumes a periodic structure of widely separated quantum wells [12]. The wavefunction of each electron or hole is described by a linear combination of bulk states

$$\psi(r) = \frac{1}{\sqrt{S}} \sum_{n,\alpha} F_{n,\alpha}(z, k_p) \mathrm{e}^{\mathrm{i}k_p x_\perp} u_\alpha(r)$$

where $u_\alpha(r)$ is the Bloch function for each subband and $F_{n,\alpha}(z, k_p)$ is an envelope function for eigenenergy E_n. The envelope function equation is given by

$$[H(z, k_p)]_\alpha [F_{n,\alpha}(z, k_p)] = E_n(k_p)[F_{n,\alpha}(z, k_p)].$$

Here square brackets denote the vector in subband α and the Hamiltonian H is described below.

The construction of the Hamiltonian is based on the method presented by Tomić *et al* [13], where the effect of adding nitrogen to the structure is modelled perturbatively because the $In_xGa_{1-x}As_{1-y}N_y$ layers have small values of y. An 8×8 Luttinger–Kohn (LK) method (coupled model of conduction, heavy, light and split-off hole bands) is used with the $In_xGa_{1-x}As_{1-y}N_y$ layers replaced by $In_{1-x}Ga_xAs$ (known as the host structure). When a small amount of nitrogen is introduced, the 8×8 Hamiltonian is expanded to a 10×10 Hamiltonian to account for coupling to the 'nitrogen band' (given by the first and sixth rows and columns in the Hamiltonian below). Additionally, some of the terms from the 8×8 contribution are modified due to the inclusion of nitrogen. The resulting 10×10 Hamiltonian is [3, 13–15]

$$H = \begin{pmatrix} E_N & V_{NC} & 0 & 0 & 0 & 0 & 0 & 0 & 0 & 0 \\ & E_C & -\sqrt{3}T_+ & \sqrt{2}U & -U & 0 & 0 & 0 & -T_- & -\sqrt{2}T_- \\ & & E_{HH} & \sqrt{2}S & -S & 0 & 0 & 0 & -R & -\sqrt{2}R \\ & & & E_{LH} & Q & 0 & T_+^* & R & 0 & \sqrt{3}S \\ & & & & E_{SO} & 0 & \sqrt{2}T_+^* & \sqrt{2}R & -\sqrt{3}S & 0 \\ & & & & & E_N & V_{NC} & 0 & 0 & 0 \\ & & & & & & E_C & -\sqrt{3}T_- & \sqrt{2}U & -U \\ & & & & & & & E_{HH} & \sqrt{2}S^* & -S^* \\ & & & & & & & & E_{LH} & Q \\ & & & & & & & & & E_{SO} \end{pmatrix} \quad (1)$$

where the subscripts N, C, HH, LH and SO stand for nitrogen, conduction, heavy-hole, light-hole and split-off bands, respectively. We do not show the lower triangle as this matrix is Hermitian. The diagonal terms of the 8×8 component of this Hamiltonian are [13, 16]

$$E_C = E_{C0} + \frac{\hbar^2}{2m_0} s_C(k_\parallel^2 + k_z^2) - (\alpha - \kappa)y$$

$$E_{HH} = E_{HH0} - \frac{\hbar^2}{2m_0}((\gamma_1 + \gamma_2)k_\parallel^2 + (\gamma_1 - 2\gamma_2)k_z^2) + \kappa y$$

Table 1. Parameters used in the calculations.

β	1.675 eV
γ	3.5 eV
κ	3.5 eV
α	1.75 eV

$$E_{\mathrm{LH}} = E_{\mathrm{LH0}} - \frac{\hbar^2}{2m_0}((\gamma_1 - \gamma_2)k_{\parallel}^2 + (\gamma_1 + 2\gamma_2)k_z^2) + \kappa y$$
$$E_{\mathrm{SO}} = E_{\mathrm{SO0}} - \frac{\hbar^2}{2m_0}\gamma_1(k_{\parallel}^2 + k_z^2) + \kappa y.$$

Here the first terms on the right-hand side of these equations represent the band-edge energies of the host system, which are found using a band-offset model that incorporates strain [13, 16]. The last terms on the right-hand side of these equations represent the modification due to the nitrogen band, y is the fraction of N in the structure, α and κ are parameters which are chosen to be 1.75 and 3.5, respectively [13]. The term $s_{\mathrm{C}} = 1/m_{\mathrm{C}}^* - (E_{\mathrm{P}}/3)[2/E_{\mathrm{g}} + 1/(E_{\mathrm{g}} + \Delta_{\mathrm{SO}})]$ is used in place of $1/m_{\mathrm{C}}^*$ and the Luttinger coefficients are replaced by $\gamma_1 \to \gamma_1 - E_{\mathrm{P}}/(3E_{\mathrm{g}}^{\mathrm{h}})$, $\gamma_{2,3} \to \gamma_{2,3} - E_{\mathrm{P}}/(6E_{\mathrm{g}}^{\mathrm{h}})$ in the 8×8 model (E_{P} and $E_{\mathrm{g}}^{\mathrm{h}}$ are the optical matrix parameter and bandgap of the host material, respectively). The other 8×8 terms are standard [16]

$$T_{\pm} = \frac{1}{\sqrt{6}}P(k_x \pm \mathrm{i}k_y)$$
$$U = \frac{1}{\sqrt{3}}Pk_z$$
$$S = \sqrt{\frac{3}{2}}\frac{\hbar^2}{m_0}\gamma_3 k_z(k_x - \mathrm{i}k_y)$$
$$R = \frac{\sqrt{3}}{2}\frac{\hbar^2}{2m_0}[(\gamma_2 + \gamma_3)(k_x - \mathrm{i}k_y)^2 - (\gamma_3 - \gamma_2)(k_x + \mathrm{i}k_y)^2]$$
$$Q = -\frac{\hbar^2}{m_0}\left(\frac{1}{\sqrt{2}}\gamma_2 k_{\parallel}^2 - \sqrt{2}\gamma_2 k_z^2\right) - \sqrt{2}\eta_{ax}$$

with P being the Kane matrix element for the conduction band and the last term in the expression for Q is the shear strain component [13, 16]. The N band components of the Hamiltonian are

$$E_{\mathrm{N}} = E_{\mathrm{N0}} + \delta E_{\mathrm{N}}^{\mathrm{hy}} - (\gamma - \kappa)y \tag{2}$$

where E_{N0} is the band-edge of the N band, including strain (which is just the hydrostatic component). Table III of Choulis *et al* [17] gives material data for InN and GaN systems. The difference between the unstrained conduction and N energy bands of 0.485 eV has been taken from Tomic *et al* [13]. V_{NC} is the only N band coupling term. It describes the interaction between the N and C bands and is given by

$$V_{\mathrm{NC}} = -\beta\sqrt{y}. \tag{3}$$

Values for γ and β are 3, 5 and 1.675, respectively [13]. The set of parameters used in the present paper is the same as the parameters used previously when analysing properties of a single quantum well [3, 13] (see table 1 for details).

Calculating the band structures of $\mathrm{In}_x\mathrm{Ga}_{1-x}\mathrm{As}_{1-y}\mathrm{N}_y$/GaAs is a two-step process:

(1) Select parameters of 'host structure' $\mathrm{In}_x\mathrm{Ga}_{1-x}$As/GaAs where we use standard ternary interpolation methods for the parameters of $\mathrm{In}_x\mathrm{Ga}_{1-x}$As.

(2) Add perturbative corrections to these due to the fraction y of N in the structure.

2.2. Self-consistent procedure

The self-consistent method is similar to the one which we used before [18] which consists of a self-consistent solution of the Poisson's equation with the matrix Schrödinger equation described by the Hamiltonian (1). The Poisson equation is

$$\frac{\mathrm{d}}{\mathrm{d}z}\left[\varepsilon(z)\frac{\mathrm{d}}{\mathrm{d}z}\phi(z)\right] = -e[\rho_{\mathrm{HH}}(z) + \rho_{\mathrm{LH}}(z) - \rho_{\mathrm{C}}(z)] \tag{4}$$

where e is the fundamental charge, $\varepsilon(z)$ is the position-dependent permittivity, $\rho_{\mathrm{C}}(z)$, $\rho_{\mathrm{HH}}(z)$ and $\rho_{\mathrm{LH}}(z)$ are the position-dependent electron and hole band density distributions, respectively. The function $\phi(z)$ is the electrostatic potential. The density distributions are [18]

$$\rho_\alpha(z) = \frac{k_{\mathrm{B}}T}{\pi\hbar^2}\left\{\sum_n \overline{m}^*_\alpha |F^{\mathrm{p}}_{n,\alpha}(z)|^2 \ln\left[1 + \exp\left(\frac{E^{\mathrm{f}}_\alpha - E^{\mathrm{p}}_{n,\alpha}}{k_{\mathrm{B}}T}\right)\right]\right\}. \tag{5}$$

The symbol α represents the conduction (C), heavy-hole (HH) and light-hole (LH) bands and n is an index over the subbands. $E^{\mathrm{f}}_{\mathrm{C}}$ is the conduction band Fermi level and $E^{\mathrm{f}}_{\mathrm{HH}} = E^{\mathrm{f}}_{\mathrm{LH}}$ is the valence band Fermi level. Their values are determined by the standard methods [16]. The symbol k_{B} is the Boltzmann constant, T is temperature and $\overline{m}^*_\alpha$ is the average effective mass for the particular band which is as approximated as the effective mass in the well since most of the carriers are confined there. Here, $F^{\mathrm{p}}_{n,\alpha}(z)$ and $E^{\mathrm{p}}_{n,\alpha}$ are the respective envelope eigenfunctions and eigenvalues of the various subbands in the *parabolic approximation* at the band-edge.

2.3. In-plane effective mass calculations

To evaluate the in-plane effective mass for the holes we look for the best fit of parabolic dispersion curves to the LK dispersion curves, with effective mass as the fitting parameter. We use an iterative routine which guesses at effective masses, compares the resulting parabolic dispersion using this effective mass near the band-edge to the 10×10 LK dispersion results using a least squares method and then refines this guess to the desired accuracy. We took the $k = 0$ energies found from the 10×10 model as the $k = 0$ energies of a parabolic model

$$E^{\mathrm{p}}_{n,\alpha}(k) = E^{10\times10}_n(0) + \frac{\hbar^2}{2m^*_{n,\alpha}}k^2 \tag{6}$$

where n denotes the nth hole band (in order energetically). The fitting parameter is then the band's effective mass $m^*_{n,\alpha}$.

In addition to finding the effective mass of each hole subband, we also classify each hole type (α) as either heavy-hole or light-hole. The procedure for this classification is as follows. Each subband wavefunction is an eigenfunction of Hamiltonian (1) and will therefore have contributions of all the N, C, HH, LH and SO bands. However, for the hole energy levels considered, the dominant contributions will only be from the LH and HH bands. If the subband under consideration, at the band-edge, has a larger LH contribution than HH it is classified to be of the LH type, otherwise it is classified as the HH type. This classification should only be taken as a rough approximation, as band mixing means we will not have pure LH or HH states. The farther we are away from the band-edge, the greater the band-mixing. Also, only the 4×4 LK approximation gives pure subband states at the band-edge. For 6×6 and greater there will be band-mixing even at the band-edge.

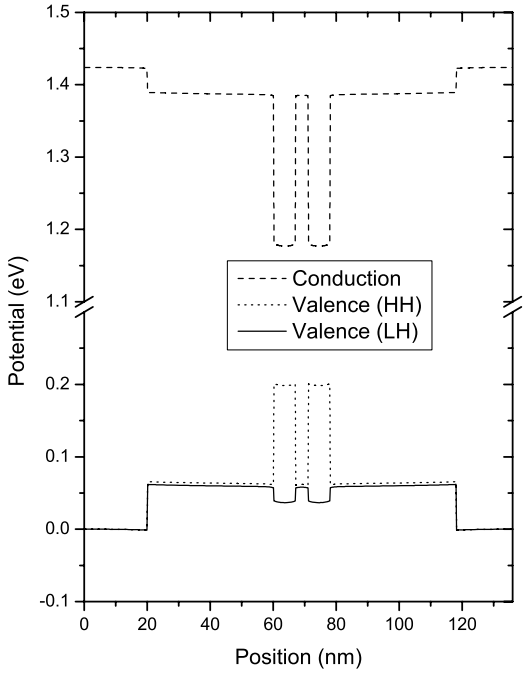

Figure 1. The heterostructure potential versus position for a separation barrier width of 2 nm and an average carrier density in the well equal to 4×10^{18} cm^{-3}.

Table 2. Heterostructure used in the calculations.

Thickness	Material	Description
'Infinite'	GaAs	Cladding
40 nm	$In_{0.05}Ga_{0.95}As_{0.985}N_{0.015}$	Barrier
7 nm	$In_{0.38}Ga_{0.62}As_{1-x}N_x$	Well
$1 \rightarrow 4$ nm	$In_{0.05}Ga_{0.95}As_{0.985}N_{0.015}$	Barrier
7 nm	$In_{0.38}Ga_{0.62}As_{1-x}N_x$	Well
40 nm	$In_{0.05}Ga_{0.95}As_{0.985}N_{0.015}$	Barrier
'Infinite'	GaAs	Substrate

3. Results

We performed our analysis for a double quantum well system as described in table 2. The structure consists of two identical quantum well separated by a barrier. We conducted our analysis for barrier widths of 1, 2, 3 and 4 nm. We also varied the nitrogen composition of both wells and considered values of nitrogen equal to 0.5, 1.0, 1.5, 2.0 and 2.5%. The wells are surrounded by 40 nm wide barriers consisting of $In_{0.05}Ga_{0.95}As_{0.985}N_{0.015}$. Outside of the structure there are GaAs cladding and substrate layers.

In figure 1 we show heterostructure potential determined in a self-consistent procedure for a 2 nm separation barrier and the average carrier density of 4×10^{18} cm^{-3}.

In figures 2 and 3 we plot the band dispersion for the first six and eight subbands of the conduction and valence bands, respectively, for a 3 nm separation barrier and well N composition $x = 1.5\%$. We see that since this is a double well system, we have close to double degeneracy for the dispersions (which gets closer to degeneracy the wider the

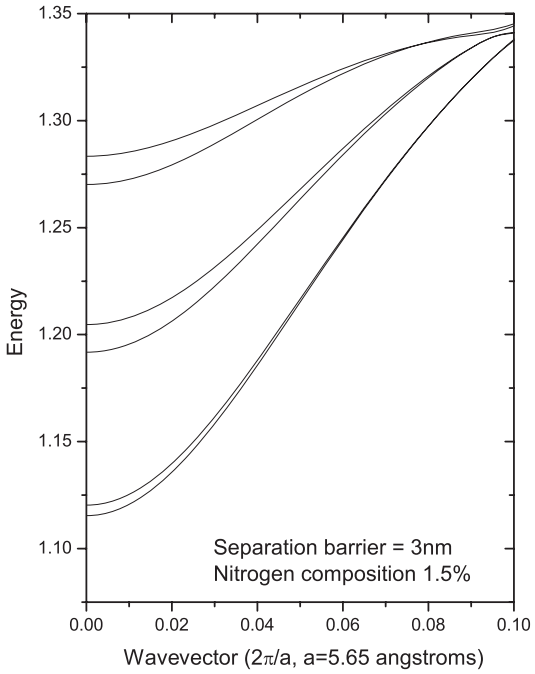

Figure 2. Band structure of electrons. Nitrogen composition 1.5%. Separation barrier equal to 3 nm.

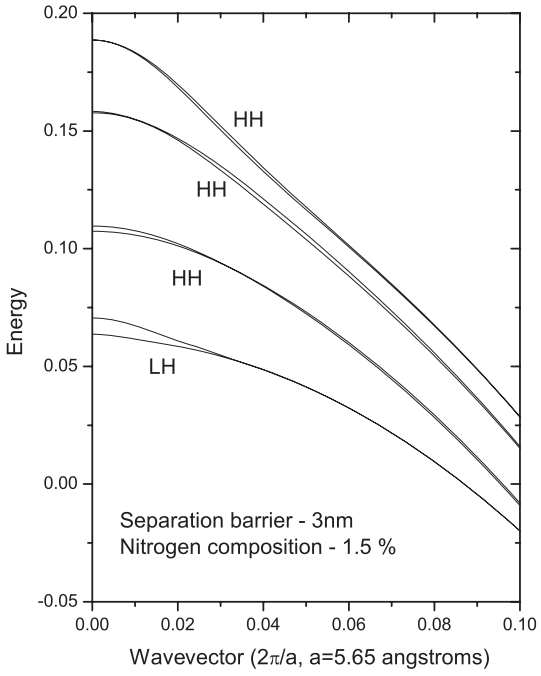

Figure 3. Band structure of holes. Nitrogen composition 1.5%. Separation barrier equal to 3 nm.

separation barrier becomes). We also label on figure 3 the subband character of each dispersion (LH or HH).

In figure 4 we plot the effective mass for the first, third, fifth and seventh subbands versus separation barrier width and well N composition of 1.5%. We choose these bands because of

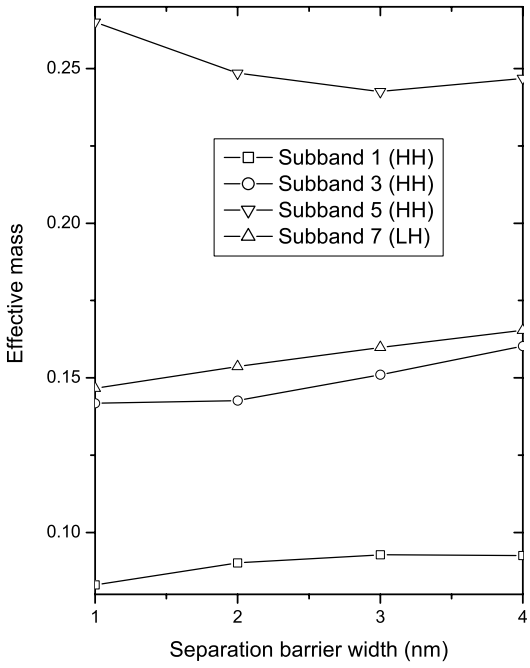

Figure 4. Effective masses versus barrier separation. nitrogen composition 1.5%.

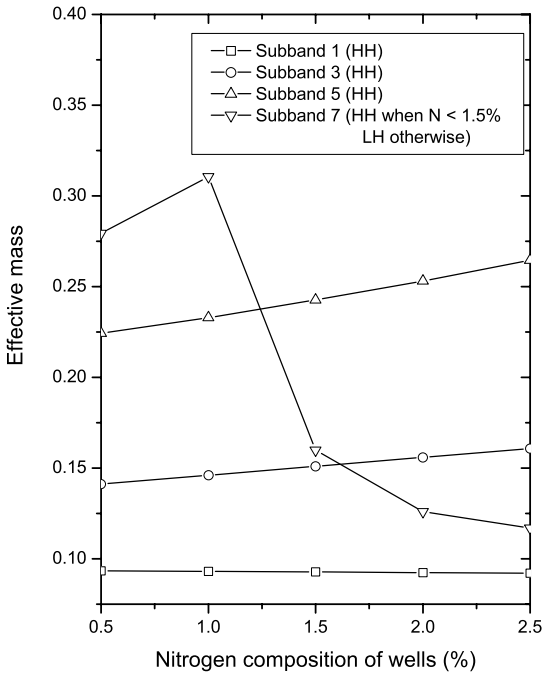

Figure 5. Effective masses versus nitrogen composition. Separation barrier equal to 3 nm.

the close double degeneracy of the levels. Subbands 1, 3 and 5 have a HH characteristic while subband 7 is closer to LH.

In figure 5 we plot the effective mass for the first, third, fifth and seventh subbands versus N composition for a barrier width of 3 nm. Again, subbands 1, 3 and 5 have a HH characteristic.

However, subband 7 is closer to HH when N $<$ 1.5% and LH otherwise. The seventh subband does not display a gradual monatomic response. Subband level 7 is greatly affected by the N composition because an examination of figures 3 and 1 shows it to be energetically close to the hole barrier's energy and N affects the well depth significantly. This level is intermediate between being free and confined.

4. Conclusions

Hole effective masses were calculated numerically for a double quantum well system in a large range of material compositions and barrier widths between quantum wells. A systematic overview has been provided. Results show that by adjusting strain and barrier width effective masses can be effectively modified. This will enable one to engineer quantum well structures for specific device requirements.

Acknowledgments

We would like to acknowledge the support from the Natural Science and Engineering Research Council of Canada (NSERC). This work was made possible by the facilities of the Shared Hierarchical Academic Research Computing Network (SHARCNET: www.sharcnet.ca). We also acknowledge comments from an anonymous referees which resulted in significant improvements to our paper.

References

[1] Klar P J 2003 *Prog. Solid State Chem.* **31** 301
[2] Alexandropoulos D and Adams M J 2002 *J. Phys.: Condens. Matter* **14** 3523
[3] Wartak M S and Weetman P 2005 *J. Phys.: Condens. Matter* **17** 6539
[4] Wartak M S and Weetman P 2005 *J. Appl. Phys.* **98** 113705
[5] Akhtar A I, Guo C-Z and Xu J M 1993 *J. Appl. Phys.* **73** 4579
[6] Akhtar A I and Xu J M 1995 *J. Appl. Phys.* **78** 2962
[7] Kucharczyk M and Wartak M S 1999 *Microw. Opt. Technol. Lett.* **21** 282
[8] Kucharczyk M, Wartak M S and Rusek P 1999 *Microw. Opt. Technol. Lett.* **22** 301
[9] Tomic S and O'Reilly E P 2005 *Phys. Rev.* B **71** 233301
[10] Tomic S, O'Reilly E P, Klar P J, Gruening H, Heimbrodt W, Chen W M and Buyanova I A 2004 *Phys. Rev.* B **69** 245305
[11] Masia F *et al* 2006 *Phys. Rev.* B **73** 073201
[12] Andreev A D and O'Reilly E P 2005 *Appl. Phys. Lett.* **87** 213106
[13] Tomic S, O'Reilly E P, Fehse R, Sweeney S J, Adams A R, Andreev A D, Choulis S A, Hosea T J C and Riechert H 2003 *IEEE J. Sel. Top. Quantum Electron.* **9** 1228
[14] Hader J, Koch S W, Moloney J V and O'Reilly E P 2000 *Appl. Phys. Lett.* **77** 630
[15] O'Reilly E P and Lindsay A 1999 *Phys. Status Solidi* b **216** 131
[16] Chuang S-L 1995 *Physics of Optoelectronic Devices* (New York: Wiley)
[17] Choulis S A, Hosea T J C, Tomic S, Kamal-Saadi M, Adams A R, O'Reilly E P, Weinstein B A and Klar P J 2002 *Phys. Rev.* B **66** 165321
[18] Weetman P and Wartak M S 2002 *Microw. Opt. Technol. Lett.* **33** 35